Supplemental Data

Endothelium-derived semaphorin 3G attenuates ischemic retinopathy by coordinating β-catenin-dependent vascular remodeling

Dan-Yang Chen,[1,2,3] Ning-He Sun,[1,2,3] Xiang Chen,[2] Jun-Jie Gong,[2] Song-Tao Yuan,[4] Zi-Zhong Hu,[4] Nan-Nan Lu,[3] Jakob Körbelin,[5] Kohji Fukunaga,[6] Qing-Huai Liu,[4] Ying-Mei Lu,[1] Feng Han[2,7]

It includes:

1. Supplemental Methods and their references
2. Supplemental Figures 1-13 and their legends
3. Supplemental Tables 1-8

Supplemental Methods

Antibodies. The following antibodies were used for immunoblotting: rabbit anti-Sema3G (1:2,000, LSBio, LS-C408533), rabbit anti-Sema3G (1:2,000, LSBio, LS-C168953), mouse anti-active-β-Catenin (1:500, Millipore, 05-665), rabbit anti-β-Catenin (1:2,000, Cell Signaling Technology, 8480), rabbit anti-phospho-β-Catenin (1:1,000, Cell Signaling Technology, 9561), rabbit anti-VE-cadherin (1:2,000, Abcam, ab33168), rabbit anti-ZO-1 (1:500, Thermo Fisher Scientific, 40-2200), mouse anti-HIF-1α (1:1,000, Abcam, ab1), rabbit anti-HIF-2α (1:1,000, Abcam, ab199), mouse anti-Flag (1:500, Sigma-Aldrich, F3165), mouse anti-β-actin (1:3,000, Cell Signaling Technology, 3700), rabbit anti-GFP (1:3,000, Abcam, ab6556), goat anti-PlexinD1 (1:1,000, Abcam, ab28762), rabbit anti-NRP2 (1:1,000, Abcam, ab273591), mouse anti-Caspase-7 (1:1,000, BD Biosciences, 551238). We used horseradish peroxidase-conjugated secondary antibodies (Jackson ImmunoResearch Laboratories) for visualization.

The following antibodies were used for tissue immunofluorescence: Fluorescein lycopersicon esculentum (tomato) lectin (1:200, Vector Laboratories, FL-1171), biotinylated Griffonia simplicifolia isolectin B4 (1:100, Vector Laboratories, B-1205), rabbit anti-Iba1 (1:500, Wako, 019-19741), mouse anti-GFAP (1:500, Millipore, MAB360), rabbit anti-Collagen IV (1:200, Abcam, ab6586), rabbit anti-Laminin (1:200, Abcam, ab11575), rabbit anti-desmin (1:50, Millipore, Ab907), rabbit anti-VE-cadherin (1:50, Cell Signaling Technology, 2158), mouse anti-active-β-Catenin (1:200, Millipore, 05-665), rat anti-TER119 (1:200, R&D Systems, MAB1125), rat anti-F4/80 (1:100, Abcam, ab6640), rat anti-PECAM-1/CD31 (1:50, BD Biosciences, 553370).

The following antibodies were used for immunocytochemistry: mouse anti-active-β-Catenin (1:200, Millipore, 05-665), rabbit anti-VE-cadherin (1:200, Abcam, ab33168), rabbit anti-ZO-1 (1:300, Thermo Fisher Scientific, 40-2200), Alexa Fluor 647 Phalloidin (1:40, Invitrogen, A22287). Alexa Fluor-conjugated secondary antibodies were from Thermo Fisher Scientific.

RNA in situ hybridization assay. Briefly, fresh 4% paraformaldehyde (PFA) was used for mouse perfusion. The retinas were dissected and fixed in PFA for another 12 h at 4°C. For hybridization in retina sections, after gradient dehydration, retinas were cut into 10 μm slices and mounted on SuperFrost Plus glass slides. Following hydrogen peroxide treatment, samples were boiled in Target Retrieval Reagent, and then the samples were incubated with protease. After digestion, Sema3G probe (Cat No. 494691, accession number NM_001025379.1), Pecam1 probe (Cat No. 316721, accession number NM_001032378.1) or Plxnd1 probe (Cat No. 405931, accession number NM_026376.3) was hybridized at 40°C for 2 h. Then, standard signal amplification was performed according to the instructions. TSA Plus Fluorescence System (PerkinElmer, NEL753001KT) was used for fluorescent detection. After the detection of mRNA, samples were further immunostained with primary antibodies and corresponding secondary antibodies. Finally, sections were stained with DAPI. Images were acquired with a Zeiss LSM800 confocal microscope (Carl Zeiss, Germany).

Immunoblotting. Samples were lysed in lysis buffer (RIPA) containing phosphatase and protease inhibitor (Thermo Fisher Scientific, 78441). The concentrations of protein were measured using a DC™ Protein Assay (Bio-Rad, 5000116) (1). Briefly, equivalent amounts of protein in lysates were separated by SDS-PAGE and transferred onto PVDF membranes.

For assessment of protein levels in patient samples, equal volumes of patient samples were loaded. Then, the PVDF membranes were incubated overnight with the respective primary antibodies at 4°C. The PVDF membranes were incubated with the appropriate secondary antibody (horseradish peroxidase-conjugated) for 1 h at RT, and immunoreactivity was detected using the ECL substrate (Amersham Biosciences, GE Healthcare). Quantification was performed using Fiji software (NIH).

Analysis of postnatal retinal angiogenesis. For vascular densities, in the superficial layer of retinas, area percentage was determined by assessing the ratio of the IB4-positive vessel area to the total measured area in a region behind the angiogenic front, and presented as a percentage of the area covered by capillary structures using ImageJ (NIH). Average vessel length was analyzed by assessing the length of individual vessels in a vascularized field, which was used to calculate the mean length in each field. In addition, in the intermediate and deep layers, the number of vessel branch points was quantified in the corresponding vessel plexus in each group (P10, P14, P20 and P60). All quantifications were calculated in a minimum of four to six fields per pup and five or more mice per group were analyzed. To determine vascular extension in the mouse retina, we calculated the ratio of the distance between the optic nerve and the developing vascular front to the radius of the whole retina. At least 8 ratio measurements were completed for each retina. The number of filopodia and sprouts were quantified at the angiogenic front of the retina. The total number of filopodia or sprouts was normalized to 1000 μm vessel length. In the retina, ECM deposits were quantified by staining with collagen IV or laminin at the angiogenic front or in remodeling plexus. Pericyte coverage was quantified by measuring the desmin-positive area

associated with the vasculature at the remodeling plexus. The number of vessel segments with discontinuous VE-cadherin labeling was quantified at the remodeling plexus. In the above quantitative statistics, the phenotype of Sema3G knockout mice was compared with those of littermate controls and mice in each group were only included if they gained bodyweight consistently (Supplemental Table 3).

Quantification of avascular area and neovascular tuft (NVT) area in OIR retinas. The retinal images were imported into Photoshop CS6 (Adobe Systems), and the area of the entire retina was traced by polygonal lasso tool and defined by the number of pixels. The avascular area was selected by quick selection tool and the number of pixels was measured. For quantification of retinal neovascularization (NV) area, the magic wand tools were used by clicking on the neovessels, and then the total number of pixels was recorded. The investigators responsible for data analysis were blinded and unaware of group allocation throughout the experiments.

Cell culture. Human retinal microvascular endothelial cells (HRMECs) were purchased from the Angio-Proteomie (CAP-0010) and cultured in complete Human Endothelial Cell Medium (Sciencell, 1001-500). For the β-catenin overexpression assay, 80% confluent HRMECs was transfected with a lentivirus carrying β-catenin coding sequence. For the hypoxic treatment, HRMECs were placed in a hypoxia chamber (Billups-Rothenberg) with 1% O_2. In the in vitro rescue experiments, Sema3G-KO HRMECs were incubated with complete Human Endothelial Cell Medium containing 200 ng/mL human recombinant Sema3G protein. For RNA interference, HRMECs were transfected with 20 nM of siRNA Duplex using lipofectamine RNAiMAX (Invitrogen, 13778100).

COS-7 (CRL-1651), HEK293 (CRL-1573) and HEK293T cells (CRL-11268) were obtained from American Type Culture Collection (ATCC) and cultured in DMEM medium (Gibco) supplemented with 10% fetal bovine serum (FBS, Gibco), streptomycin (100 μg/mL), and penicillin (100 U/mL) (Life Technologies, 15140122). For AP binding assay, 80% confluent COS-7 cells were transfected with overexpression plasmids using Lipofectamine 3000 (Invitrogen, L3000008).

Mouse cerebral microvascular ECs (bEnd.3) were obtained from ATCC (CRL-2299) and cultured in DMEM GlutaMAX (Gibco) with 10% FBS (Gibco), streptomycin (100 μg/mL), and penicillin (100 U/mL) (Life Technologies, 15140122). For the hypoxic treatment, bEnd.3 cells were placed in a hypoxia chamber (Billups-Rothenberg) with 1% O_2. For RNA interference, bEnd.3 cells were transfected with 20 nM of siRNA Duplex using Lipofectamine RNAiMAX (Invitrogen, 13778100).

Immunocytochemistry. Briefly, cells were washed and fixed at RT in 4% PFA for 15 min. PBS containing 0.1% Triton X-100 was used for permeabilization. Then, cells were blocked for 1 h in blocking buffer (3% bovine serum albumin in PBS). After blocking, cells were incubated with primary antibodies in blocking buffer at 4°C overnight. Next, cells were incubated with appropriate fluorescent secondary antibodies at RT for 2 h. Finally, cells were stained with DAPI and mounted in Vectashield medium (Vector Laboratories). Images were acquired with a Zeiss LSM800 confocal microscope (Carl Zeiss, Germany).

Plasmid construction. To knock down Sema3G in HRMECs, shSema3G or control shRNA oligo was cloned into the lentiviral vector (pLKD-U6-shRNA), in which shRNA was driven by the U6 promoter. To knock out Sema3G in HRMECs, a 23 bp target DNA sequence

containing protospacer adjacent motif (PAM) in the first exon sequence of human Sema3G genomic locus was chosen for generation of a sgRNA. To construct the sgRNA expression vector, the targeting sequence and scaffold sequence of sgRNA were subcloned into the pLKO.1 puro plasmid containing U6 promoter. After construction, the pLKO.1 puro-sgControl and pLKO.1 puro-sgSema3G plasmid was verified by DNA sequencing. Finally, pLenti-CMV-blasticidin-P2A-3 × Flag-Cas9, pLKO.1 puro-sgControl and pLKO.1 puro-sgSema3G vectors were used for further lentivirus packaging, and the lentivirus was produced by OBiO Technology (China). In addition, the human β-catenin coding sequence was synthesized by GenScript (China) and was used for overexpression vector construction. β-catenin overexpressing and empty lentiviral vector was used for lentiviral packaging.

For in vivo knockdown of PlexinD1 in retinal ECs of the OIR mice, pAAV-U6-shControl and pAAV-U6-shPlexinD1 was constructed using pAAV-U6-shRNA (NC) vector. For the in vivo overexpression of Sema3G, the PCR product of the Sema3G-3 × Flag or GFP sequence was subcloned into the pFastbac-CAG-iCre-2A-GFP expression vector (a kind gift from Dr. Jakob Körbelin, University Medical Center Hamburg-Eppendorf) by replacing the originally existing iCre-2A-GFP sequence. The above AAV vectors were verified by sequencing in Genewiz (China). These AAV vectors were respectively used with the replication-capsid packaging plasmid and helper plasmid to package AAV (2), which specifically infects central nervous system ECs. The AAV was produced by OBiO Technology (China).

For AP binding assays, the AP-Sema3F vector was a kind gift from Dr. Alex L. Kolodkin (Johns Hopkins University) for generating the AP-Sema3F fusion protein

(AP-Sema3F). To construct the AP-Sema3G expression plasmid, the coding sequence of human Sema3G was subcloned into the C-terminal of AP in a pAPtag5 vector. The PlexinD1 and Nrp2 expression vectors were kind gifts from Dr. Alex L. Kolodkin (Johns Hopkins University) for overexpression in COS-7 cells. The Nrp2 coding sequence with a Myc epitope (EQKLISEEDL) at the C-terminus was subcloned into the pcDNA3.1(+) (Invitrogen). The empty pcDNA3.1(+) vector was used as a control.

For luciferase reporter assays, pGL3-Basic vectors (E1751) were purchased from Promega, and pGL3-SV40-luciferase as a positive control was generated by inserting the SV40 promoter into multiple cloning sites (MCS) in pGL3-Basic vectors. Sema3G genomic promoter containing the 5′-flanking region, spanning from −2000 to +80 relative to the transcription start site (TSS), were amplified by PCR and then inserted into the MCS of pGL3-Basic vectors to generate WT hypoxia response element (HRE) vector. Mutations were introduced into the HRE by specific primers containing point mutations (nominated as mHRE-1, mHRE-2, mHRE-3 vectors). The vector for 5 × HRE was constructed by inserting two additional HREs into the mouse Sema3G genomic promoter region. All plasmids were confirmed by sequencing in Genewiz (China).

For in vivo Matrigel angiogenesis assay, the adenovirus vector pAdeno-mCMV-Sema3G-3 × Flag was constructed using pAdeno-mCMV-MCS-3 × Flag vector and the empty vector was used as a control. The control and Sema3G overexpression vector were used for adenovirus packaging in OBiO Technology (China).

ChIP-qPCR. Chromatin immunoprecipitation (ChIP) was performed using a Pierce Agarose ChIP Kit (Thermo Fisher Scientific, 26156). Briefly, bEnd.3 cells were cultured

under hypoxic conditions. Cells were cross-linked with fresh formaldehyde, followed by cell pellet isolation. The cross-linked cells were extracted to obtain nuclei and digested with 0.25 μL of micrococcal nuclease (10 U/μL) for generating DNA fragments in each sample. After centrifugation, the digested chromatin in the supernatant was obtained. The 10% total input containing the digested chromatin from one ChIP was used in this procedure. For each IP, the digested chromatin was incubated with 10 μg HIF-1α or HIF-2α antibody overnight at 4℃ and immunoprecipitated with ChIP Grade Protein A/G Agarose for one hour at 4℃. After incubation with agarose, the resin was washed using Wash Buffer and then eluted with Elution Buffer. Then the eluent containing the chromatin was digested with 2 μL of 20 mg/mL Proteinase K. The digested IP samples were purified with a DNA Clean-Up Column. Purified DNA was eluted with DNA Elution Solution and amplified by standard qPCR with the use of oligonucleotides flanking the promoter regions containing the HREs. For qPCR analyses in QuantStudio 5 (Applied Biosystems, USA), template DNA was mixed with specific primers (10 mM each) in AceQ qPCR SYBR Green Master Mix (Low ROX Premixed) (Vazyme, Q131-02). Finally, the fold enrichment was calculated by normalizing fold changes to the IgG control.

Luciferase reporter assays. Dual-Luciferase Reporter Assay System (Promega, E1910) was used for reporter assays according to the manufacturer's instructions. Briefly, reporter vectors (500 ng of WT HRE vector, mHRE vectors or 5 × HRE vector) were transfected with 10 ng of pRL-TK (Promega, a Renilla luciferase reporter vector) into HEK293 cells in 24-well plates using Lipofectamine 3000 (Invitrogen, L3000008). The pGL3-SV40-luciferase was chosen as a positive control. Then, 24h after transfection, the cells were cultured in a

normoxic or hypoxic environment. 48h after transfection, cells were harvested in lysis buffer for 20 min at RT. Finally, Dual-Luciferase Reporter Assay System was used to detect Firefly and Renilla luciferase activity of lysates and a microplate luminometer (BERTHOLD, Centro LB 960) was used for luminescence detection. All data were obtained from three independent experiments and relative luciferase activity was calculated by normalizing Firefly/Renilla values.

Generation of phylogenetic tree. We used Clustal Omega to analyze the distance of *Sema3s* (*Sema3, A-G*) and visualized the tree files by Figtree. Briefly, we downloaded the open reading frame sequence from the NCBI (https://www.ncbi.nlm.nih.gov/gene) as fasta files, including human or mouse *Sema3s* and *Sema3G* of different species. Then, we uploaded the fasta files to Clustal Omega and obtained the NEXUS files with default settings. PAUP4 was used to generate the tree files. Finally, Figtree was used to visualize the tree files.

Multiple sequence alignment. Sema3G protein-coding sequence files of different species were obtained from NCBI (https://www.ncbi.nlm.nih.gov/protein). Clustalw was the program used for multiple sequence alignment and generated the ".aln" files. The files were uploaded to ESPript. Then, a visual sequence similarity file was generated.

BBB permeability measurements. Neonatal pups were anesthetized with 2% isoflurane and maintained with 1.5% isoflurane. In brief, 1% biocytin-TMR solution (869 Da, Thermo Fisher Scientific, T12921) was injected through the retro-orbital sinus with a 33 gauge needle (TSK Laboratory). After circulation for 30 min, eyes were enucleated and retinas were stained with IB4. Distal vessels were referred to the field near the retinal tip cells and proximal vessels were referred to the field adjacent to the optic disc. The permeability index

was quantified as the area of the tracer divided by the area of the vessel in each image. Six areas were imaged on the superficial layer vasculature per retina and the average of the ratios is considered one biological sample. Six mice per group were studied.

Quantification of other microscopic imaging data in OIR model. All confocal images were acquired with the same parameters. Staining intensities of β-catenin and VE-cadherin in OIR retina were measured in regions of interest (ROI) of vessels in each field and averaged using ImageJ (NIH). For comparison, the values were then normalized to the average of control and displayed as a percentage. The stained area of TER119-positive cells (RBC leakage) or F4/80-positive cells (macrophage infiltration) in OIR retina was measured and averaged as a percentage of total area using the same threshold values in ImageJ (NIH). Six areas per retina were imaged and five or more mice per group were analyzed.

Lentiviral transduction. For Sema3G knockdown, HRMECs were transduced with pLKD-U6-shSema3G or control lentivirus (multiplicity of infection, MOI = 25) in 24-well plates. For Sema3G knockout using CRISPR/Cas9, HRMECs were transduced with pLenti-CMV-blasticidin-P2A-3 × Flag-Cas9 and pLKO.1 puro-sgSema3G or control lentivirus (MOI = 25) in 24-well plates. Genomic DNA of HRMECs was extracted using Genomic Miniprep Kit (Axygen, AP-MN-MS-GDNA-250) after transduction of Cas9 and sgRNA lentivirus. The genomic sequence around the target Sema3G DNA site was amplified by PCR. Then, the PCR products were separated in 2.0% agarose gel and purified for sequencing.

Alkaline phosphatase (AP) binding assays. HEK293T cells were transfected with

AP-tagged Sema3G or AP-tagged Sema3F vectors. The corresponding supernatant was collected, filtered and concentrated using Amicon Ultra Filters (Millipore). Then, the supernatant was mixed with AP substrate buffer (15 mL of 2 M diethanolamine containing 15 μL of 1 M $MgCl_2$ and 100 mg of p-nitrophenyl phosphate, pH 9.8), and the change in absorbance of the resulting mixture at 405 nm (optical density units per hour) was measured by a spectrophotometer to indicate AP activity.

For binding assays in cells (3), HRMECs were transfected with siControl, siPlexinD1 alone, siNrp2 alone or siPlexinD1 with siNrp2. In addition, COS-7 cells were transfected with control, PlexinD1 alone, Nrp2-Myc alone or PlexinD1 with Nrp2 overexpression vectors. After incubating with AP-Sema3F (2 nM) or AP-Sema3G (2 nM) for 90 min at RT, cells were washed with cold HBAH buffer (20 mM HEPES, 0.1% NaN_3, 0.5 mg/mL BSA, pH 7.0) and then fixed for 5 min in 4% PFA. For inactivating endogenous AP activity, the cells were washed with HBS (20 mM HEPES, 150 mM NaCl, pH 7.0) and incubated at 65°C for 1 h. Finally, 5-bromo-4-chloro-3-indolyl-phosphate (BCIP)/nitroblue tetrazolium (NBT) was used to analyze the in situ bindings of AP fusion protein on the cell surface.

Immunoprecipitation. Capturem IP & Co-IP Kit (Takara, 635721) was used for extracting protein-protein complexes from cell lysates. Briefly, cells were washed with PBS and lysed for 15 min on ice using 600 μL of lysis/equilibration buffer with protease inhibitors (Roche). Next, cell lysates were centrifuged at 4°C for 10 min. 50 μL of lysate was used as the input. The remaining lysates were incubated with the corresponding primary antibody or IgG at 4°C for 2 h. Then, the sample was loaded onto the spin column and centrifuged. The spin column was washed with wash buffer and centrifuged. Immunoprecipitated proteins

were eluted with elution buffer. Finally, immunoprecipitates and cell lysates were further analyzed by immunoblotting.

RNA sequencing and gene expression analysis. Total RNA in control and Sema3G-silenced HRMECs were extracted using RNAiso Plus (TaKaRa), followed by quality control with an Agilent 2100 Bioanalyzer (Agilent Technologies). Qualified samples were chosen for next-generation sequencing library preparation using the NEBNext Ultra RNA Library Prep Kit. Then, DNA sequencing of the libraries was performed on an Illumina platform and data were processed by Genewiz (China). In order to remove adapters and low-quality reads, data of fastq format were performed by Cutadapt (V1.9.1) to be clean data. Annotation files and reference genome sequences of homo sapiens were obtained from ENSEMBL. Then, the clean data were aligned to reference genome sequences using Hisat2 (v2.0.1). The gene expression levels from the pair-end clean data were estimated using HTSeq (v0.6.1). DESeq2 bioconductor package was used for differential gene expression analysis between two groups. DESeq2 estimated each gene expression by linear regression and then calculated the p-value corrected by the BH method. Differentially expressed genes (DEGs) between two groups were characterized by $q \leq 0.05$ and $|\log_2 \text{Foldchange}| \geq 1$. GOSeq (v1.34.1) was used for identifying Gene Ontology (GO) terms. Kyoto Encyclopedia of Genes and Genomes (KEGG) analysis of DEGs was evaluated via a Genewiz-written script.

Laser-induced choroidal neovascularization (CNV) model. P20 and P60 male mice were used for generation of CNV model according to a previously established method (4). After topical treatment with 1% tropicamide for pupillary dilation and 0.5% proparacaine

hydrochloride (Alcon) for topical anesthesia, laser burns were made with a laser photocoagulator (Novus Varia, LUMENIS) with a slit lamp delivery system. An artificial tear adhered glass coverslip was used as a contact lens. The laser system was setting to parameters: 50 μm spot size, 100 ms duration, 150 mW power, 532 nm wavelength, and laser was delivered ideally at the 3, 6, 9, and 12 o'clock positions around the optic disc. There would be a bubble formation immediately when properly focused and burned in Bruch's membrane. Spots with hemorrhage caused by laser were not included in the statistics. In each experimental group, 10 mice with four impacts per eye were analyzed to overcome the inherent variability.

For fluorescein angiography (FA) and indocyanine green angiography (ICGA) of the CNV lesion, 5 mg of fluorescein sodium (50 mg/mL) and 0.15 mg of indocyanine green (1 mg/mL) were administered intraperitoneally or intravenously on day 14 after laser injury, respectively. The mice were imaged 6 minutes after injection using a confocal laser scanning system (Heidelberg Spectralis HRA2). For quantification of leaky areas from CNV, the total hyperfluorescent areas in FA images were divided by the total CNV areas in ICGA images using ImageJ (NIH).

For quantification of CNV volume, mice were euthanized on day 14 after laser injury, and flat-mounted choroids (5) were stained with IB4 to label the CNV vessels and analyzed (three-dimensions, 3D) with Imaris software (Bitplane, Switzerland).

In vivo Matrigel angiogenesis assay. C57BL/6 mice were anesthetized with 3% isoflurane and maintained with 1.5% isoflurane. The mice were injected subcutaneously with 200 μL Matrigel (BD Biosciences, 356237) as described (6, 7). Matrigel was mixed with 80

ng/mL recombinant mouse bFGF (R&D Systems, 3139-FB-025) or with 100 ng/mL recombinant murine $VEGFA_{165}$ (Peprotech, 450-32) containing 1×10^9 plaque-forming unit adenovirus expressing Sema3G-3 × Flag protein or control adenovirus. After 7 days, 100 μL of a 1:1 mixture of 10 mg/mL dextran-fluorescein (dextran-FITC, 2,000,000 MW, Thermo Fisher Scientific, D7137) and dextran-tetramethylrhodamine (dextran-TRITC, 10,000 MW, Thermo Fisher Scientific, D1868) was intravenously injected into mice. After circulating for 15 min, the plugs were harvested.

For immunostaining of Matrigel plugs, plugs were fixed in 4% PFA at 4°C for 12 h. Then, the plugs were embedded in OCT embedding medium (Tissue-Tek), sectioned into 45 μm slices on a freezing microtome (Leica) and mounted on SuperFrost Plus glass slides (Thermo Fisher Scientific) for immunostaining. NikonA1R confocal microscope was used for z-stack image acquisition. Imaris software (Bitplane, Switzerland) was used to render the 3D images of vessels in plugs. The percentage of area (P) of dextran-TRITC tracer extravasation was measured by the following formula: $P_{(\text{TRITC outside vessels})} = P_{(\text{Area corresponding to the dextran-TRITC tracer})} - P_{(\text{Area corresponding to the dextran-FITC tracer})}$.

References for supplemental methods

1. Chen DY, et al. GPR124 facilitates pericyte polarization and migration by regulating the formation of filopodia during ischemic injury. *Theranostics.* 2019;9(20):5937-5955.

2. Korbelin J, et al. A brain microvasculature endothelial cell-specific viral vector with the potential to treat neurovascular and neurological diseases. *EMBO Mol Med.* 2016;8(6):609-625.

3. Tran TS, et al. Secreted semaphorins control spine distribution and morphogenesis in the postnatal CNS. *Nature.* 2009;462(7276):1065-1069.

4. Lambert V, et al. Laser-induced choroidal neovascularization model to study age-related macular degeneration in mice. *Nat Protoc.* 2013;8(11):2197-2211.

5. Claybon A, Bishop AJ. Dissection of a mouse eye for a whole mount of the retinal pigment epithelium. *J Vis Exp.* 2011(48).

6. Birdsey GM, et al. Transcription factor Erg regulates angiogenesis and endothelial apoptosis through VE-cadherin. *Blood.* 2008;111(7):3498-3506.

7. Birdsey GM, et al. The endothelial transcription factor ERG promotes vascular stability and growth through Wnt/beta-catenin signaling. *Dev Cell.* 2015;32(1):82-96.

Supplemental Figures

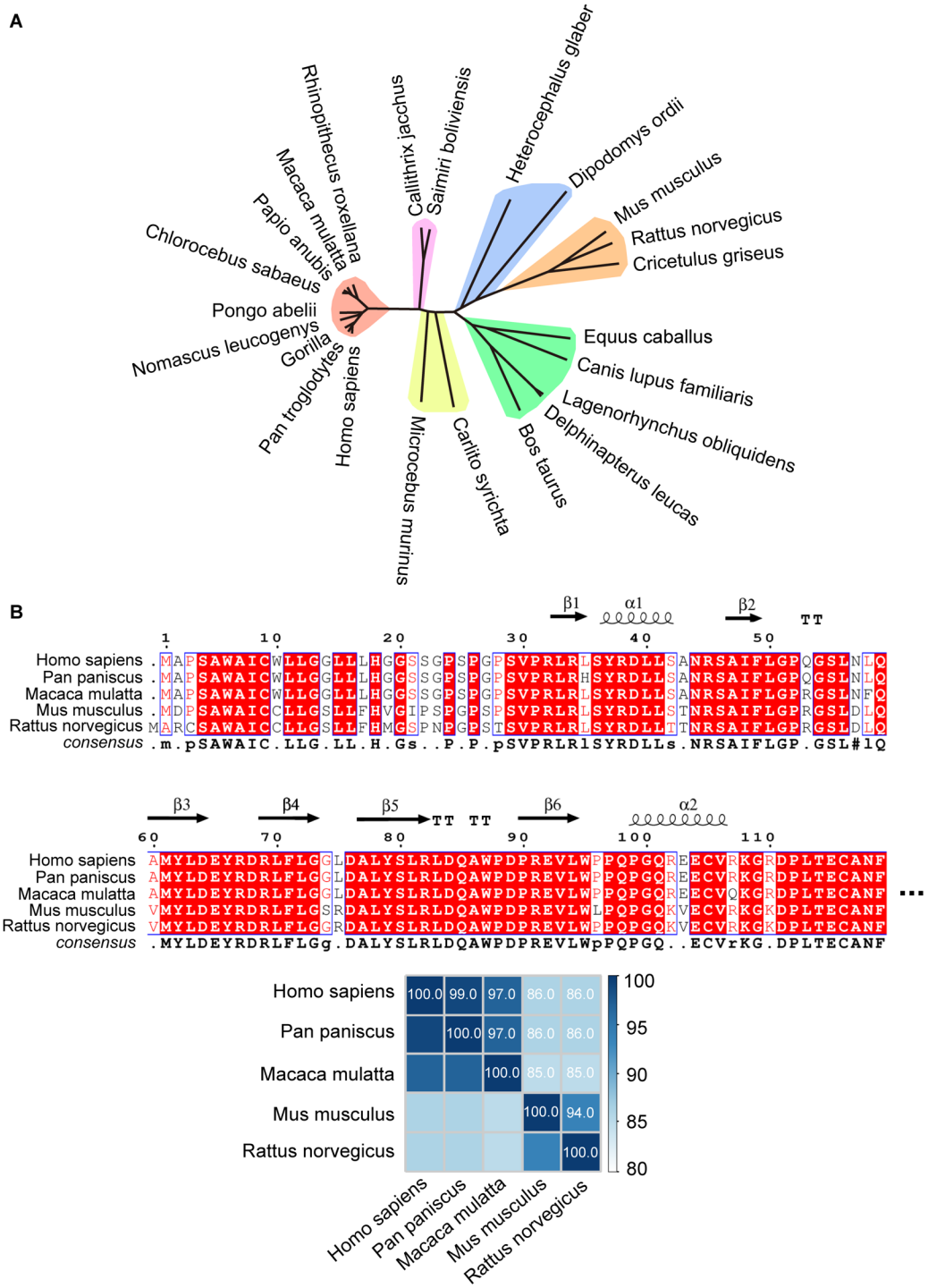

Supplemental Figure 1. Sema3G is evolutionarily conserved among various species. (**A**) The phylogenetic tree was constructed with Figtree. The *Sema3G* from different species were clustered and divided into distinct subfamilies. (**B**) Representative sequence alignment of Sema3G conserved residues from different species.

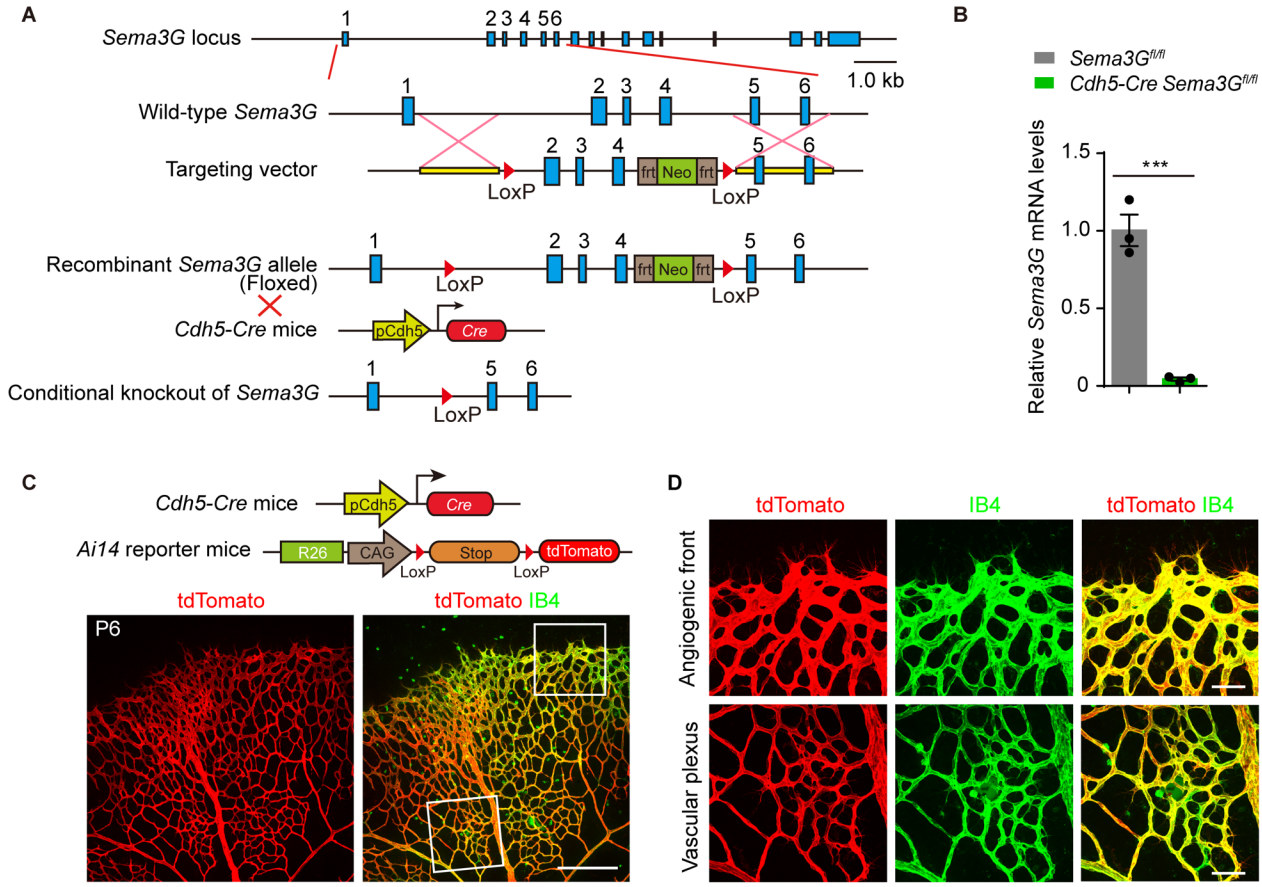

Supplemental Figure 2. High knockout efficiency of Sema3G in retinal vessels is achieved by Cre-mediated recombination using *Cdh5-Cre* mice. (**A**) Schematic illustration of the *Sema3G* gene, the targeting vector and the floxed *Sema3G* locus. Floxed *Sema3G* transgenic mice (*Sema3G*$^{fl/fl}$) were bred with the *Cdh5-Cre* mouse line (Cre expressed under the control of the Cdh5 promoter) to generate *Sema3G* endothelial cell conditional knockout mice (*Cdh5-Cre Sema3G*$^{fl/fl}$ mice). (**B**) Relative mRNA levels of *Sema3G* in retinal ECs of *Sema3G*$^{fl/fl}$ and *Cdh5-Cre Sema3G*$^{fl/fl}$ mice (n = 3 mice). (**C** and **D**) *Cdh5-Cre* mice crossed with *Ai14* reporter mice. Images of IB4-positive retinal vessels at the angiogenic front and vascular plexus in *Cdh5-Cre Ai14* mice at P6 and higher magnification images of the boxed region are displayed. tdTomato is expressed in most IB4-positive retinal vessels (> 90%). Error bars represent mean ± SEM. ***P<0.001; 2-tailed Student's t tests. Scale bars: 200 μm (**C**) and 50 μm (**D**).

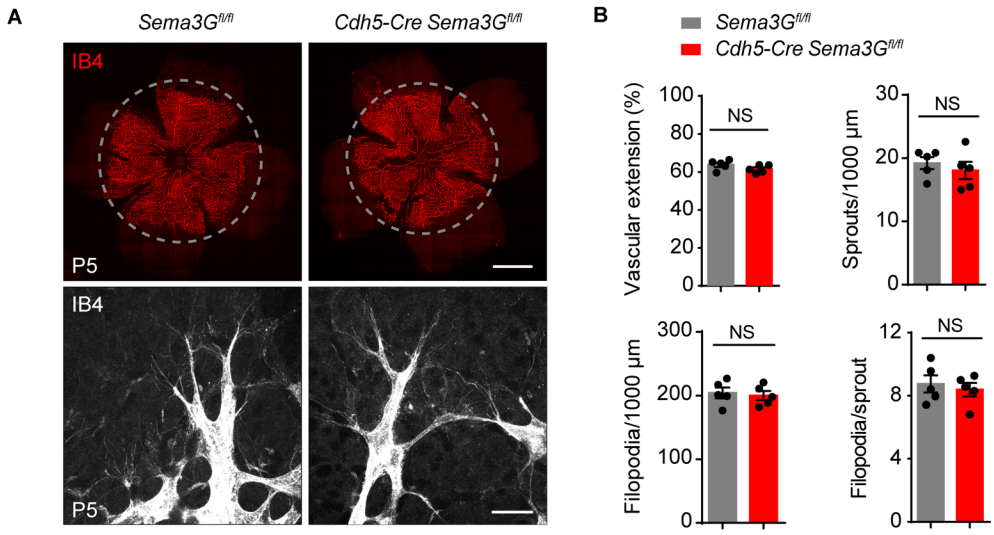

Supplemental Figure 3. Endothelial Sema3G deletion has no effect on vascular sprouting and filopodia formation. (**A**) Representative low-magnification image of IB4-stained retinas (upper panel) and the high-resolution image showing the emergence of sprouts and filopodia at the angiogenic front (lower panel) of *Sema3G$^{fl/fl}$* and *Cdh5-Cre Sema3G$^{fl/fl}$* at P5. The gray dashed circle represents the vascular outgrowth of the retina. (**B**) Quantification of the ratio of vascular extension, the number of sprouts per 1000 µm vessel length, the number of filopodia per 1000 µm vessel length and the ratio of filopodia to sprouts (n = 5 mice). Error bars represent mean ± SEM. 2-tailed Student's t tests. Scale bars: 1000 µm (**A**, upper panel) and 25 µm (**A**, lower panel).

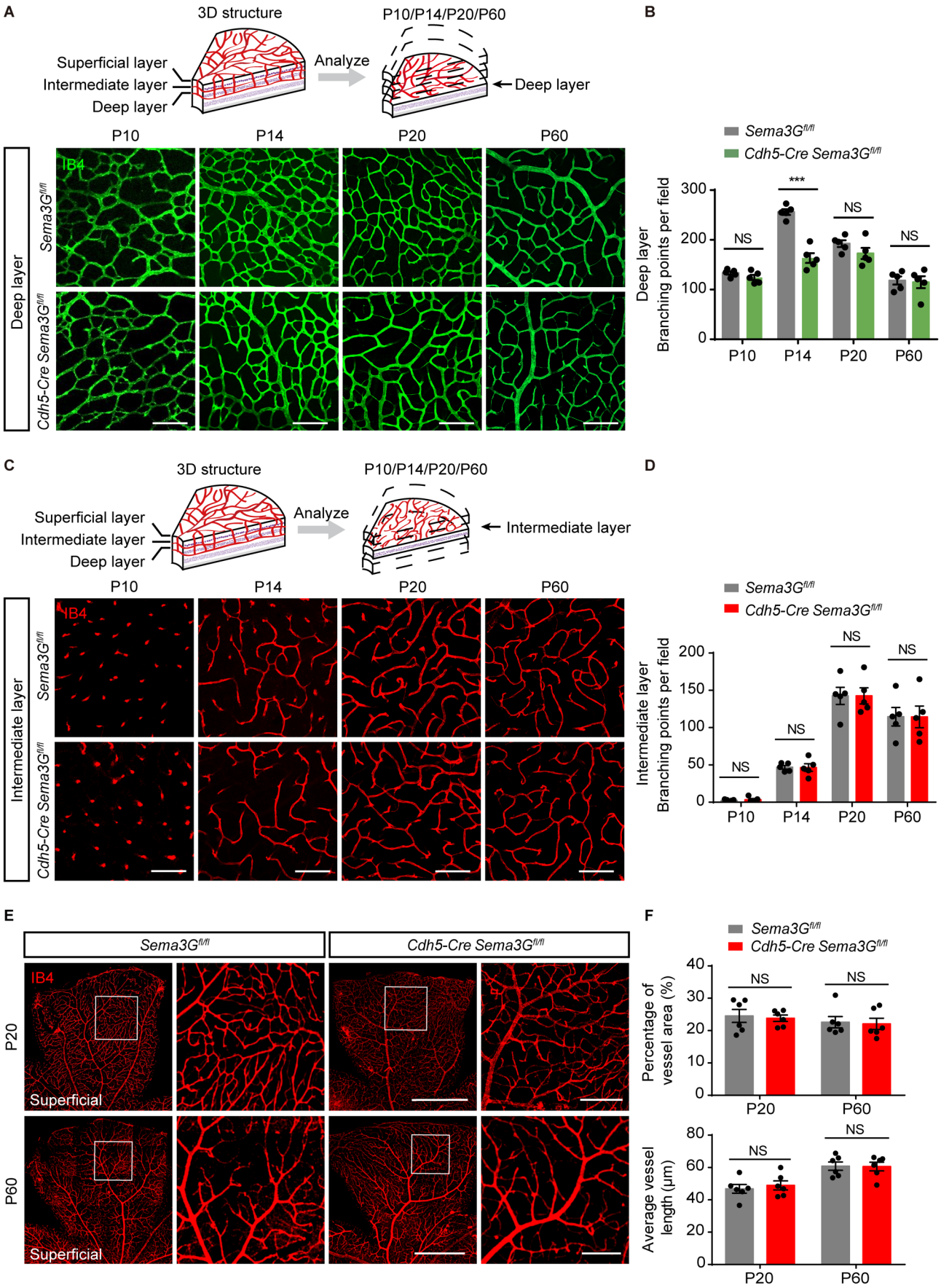
A
3D structure
P10/P14/P20/P60
Superficial layer
Intermediate layer
Deep layer
Analyze
Deep layer
P10
P14
P20
P60
Deep layer
IB4
Sema3G fl/fl
Cdh5-Cre Sema3G fl/fl
B
Sema3G fl/fl
Cdh5-Cre Sema3G fl/fl
Deep layer Branching points per field
***
NS
C
3D structure
P10/P14/P20/P60
Superficial layer
Intermediate layer
Deep layer
Analyze
Intermediate layer
Intermediate layer
D
Intermediate layer Branching points per field
E
Sema3G fl/fl
Cdh5-Cre Sema3G fl/fl
P20
P60
IB4
Superficial
F
Percentage of vessel area (%)
Average vessel length (μm)

Supplemental Figure 4. Endothelial Sema3G deletion has no effect on the vascular network at the later stage in development. (**A**) IB4-positive blood vessels in the deep layer of the retina at P10, P14, P20, and P60. (**B**) Quantification of branching points per field in the deep layer of the retina at P10, P14, P20, and P60 (n = 5 mice). (**C**) IB4-positive blood vessels in the intermediate layer of the retina at P10, P14, P20, and P60. (**D**) Quantification of branching points per field in the intermediate layer of the retina at P10, P14, P20, and P60 (n = 5 mice). (**E**) Superficial IB4-positive blood vessels of P20 and P60 retinas. Higher magnification images of the boxed region are displayed in the right panel. (**F**) Quantification of percentage of vessel area and average vessel length of P20 and P60 retinas (n = 6 mice). Error bars represent mean ± SEM. ***P<0.001; 2-tailed Student's t tests. Scale bars: 100 μm (**A** and **C**) and 1000 μm (**E**); magnified images, 200 μm (**E**).

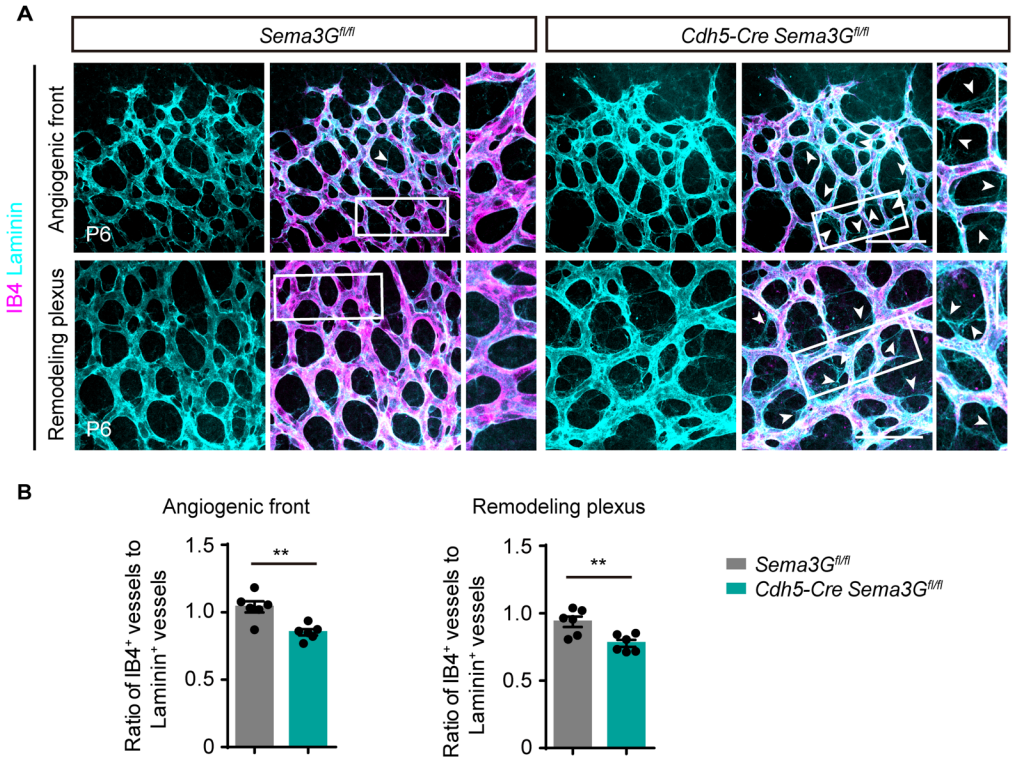

Supplemental Figure 5. Retinas of Sema3G knockout mice exhibit excessive vascular ECM deposition. (**A**) Confocal images of P6 whole-mount retinas immunostained with antibodies detecting laminin as indicated (cyan) at the angiogenic front (upper panel) and in the remodeling plexus (lower panel). (**B**) Quantification of the ratio of IB4-positive vessels to Laminin-positive vessels at the P6 angiogenic front (left, *Sema3G*$^{fl/fl}$, n = 6 mice; *Cdh5-Cre Sema3G*$^{fl/fl}$, n = 6 mice) and in the remodeling plexus (right, *Sema3G*$^{fl/fl}$, n = 6 mice; *Cdh5-Cre Sema3G*$^{fl/fl}$, n = 6 mice). Error bars represent mean ± SEM. **P<0.01; 2-tailed Student's t tests. Scale bars: 100 μm (**A**); magnified images, 50 μm (**A**).

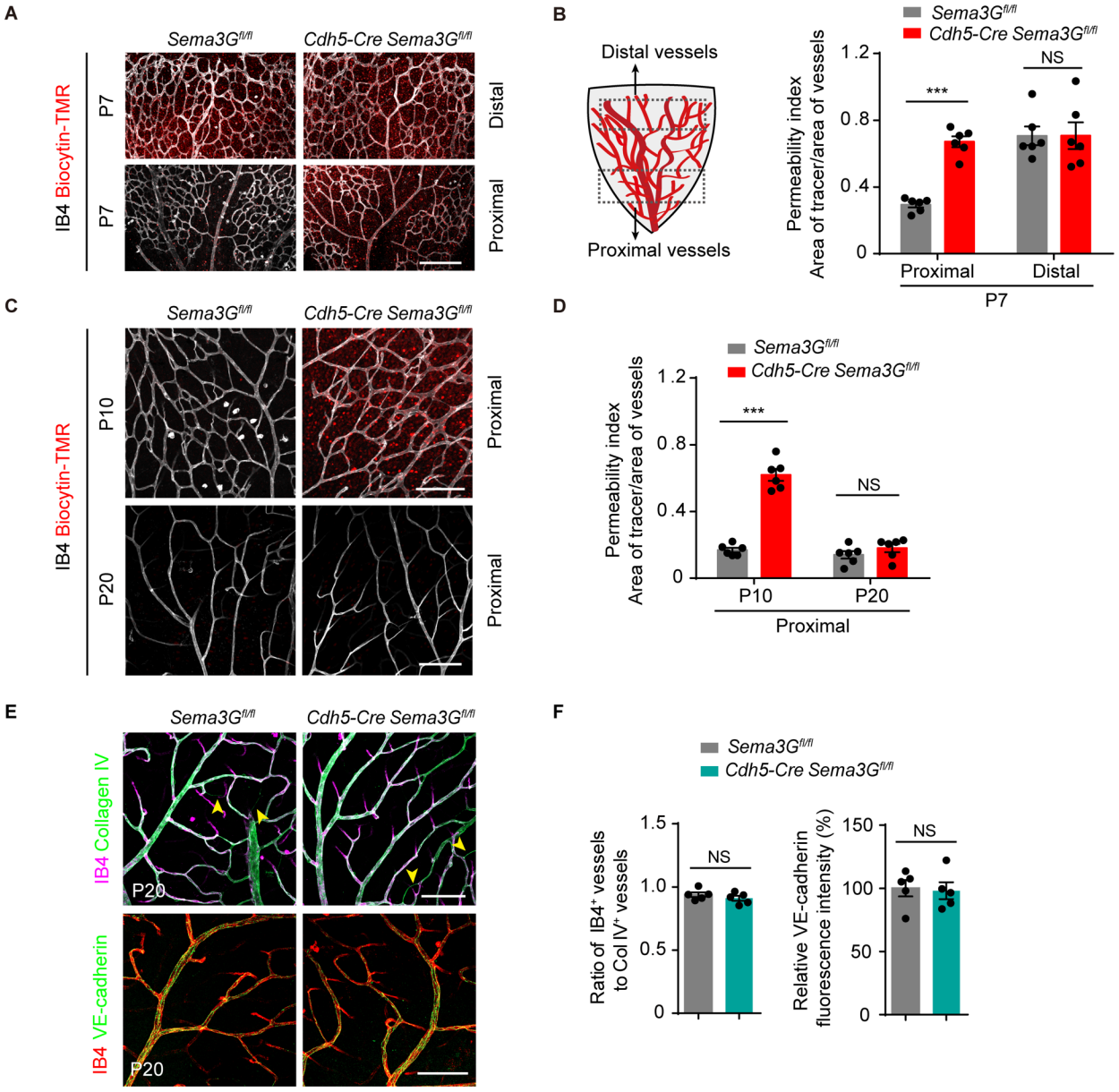

Supplemental Figure 6. Sema3G is essential for BRB formation in the remodeling plexus. (**A** and **C**) Representative images of *Sema3G*$^{fl/fl}$ and *Cdh5-Cre Sema3G*$^{fl/fl}$ retinas at P7 (**A**), P10 (upper panel in **C**), and P20 (lower panel in **C**) following injection of biocytin-TMR into mice. (**B** and **D**) Quantitation of the permeability index of biocytin-TMR at P7 (**B**), P10 and P20 (**D**) (n = 6 mice for each group). Distal vessels were referred to the field near the retinal tip cells and proximal vessels were referred to the field adjacent to the optic disc. (**E**) Representative images showing collagen IV (green)-positive but IB4 (magenta)-negative matrix sleeves (yellow arrowheads) in the vascular plexus of P20 mice (upper panel). Confocal images of anti-VE-cadherin (green)- and IB4 (red)-stained vascular plexus in P20 retinas (lower panel). (**F**) Quantification of the ratio of IB4-positive vessels to collagen IV-positive vessels in the P20 plexus (n = 5 mice for each group) and quantitation of the fluorescence signal intensity of junctional VE-cadherin (n = 5 mice for each group). Error bars represent mean ± SEM. ***P < 0.001; 2-tailed Student's t tests. Scale bars: 200 μm (**A**) and 100 μm (**C** and **E**).

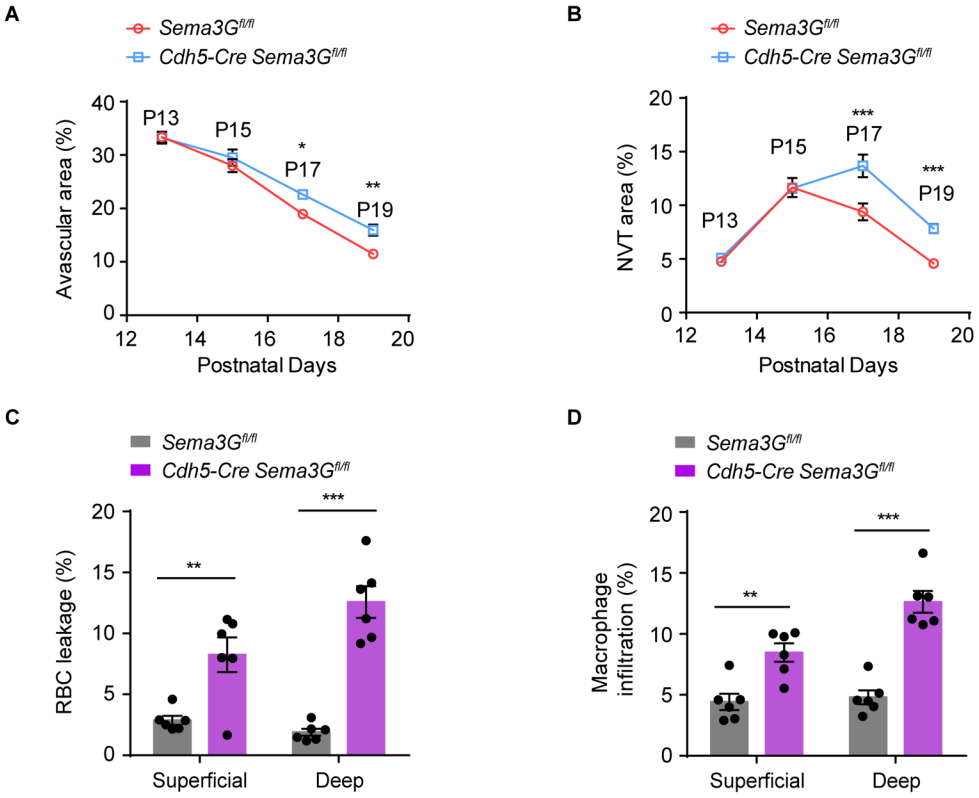

Supplemental Figure 7. Loss of Sema3G aggravates pathological angiogenesis in OIR mice. (**A** and **B**) Comparisons of the avascular area and NVT area at various time points during OIR. (**C** and **D**) Quantitation of RBC leakage and macrophage infiltration in superficial and deep retinal layers of *Sema3G*$^{fl/fl}$ OIR and *Cdh5-Cre Sema3G*$^{fl/fl}$ OIR mice, related to Figure 6, **I** and **J** (**C**, n = 6 mice for each group; **D**, n = 6 mice for each group). Error bars represent mean ± SEM. *P<0.05; **P<0.01; ***P<0.001; 2-way ANOVA with Bonferroni's multiple comparisons test (**A** and **B**), 2-tailed Student's t tests (**C** and **D**).

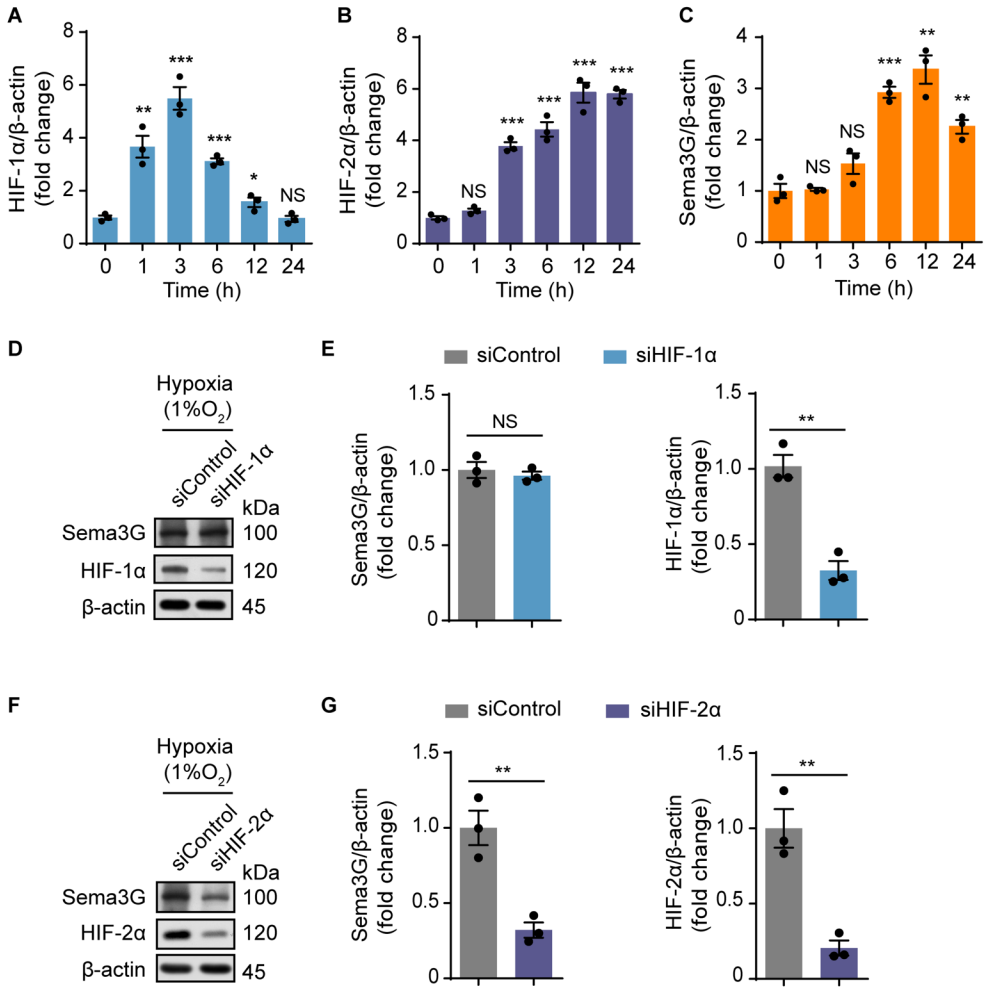

Supplemental Figure 8. HIF-2α regulates Sema3G expression upon hypoxia in ECs. (**A-C**) Quantification of HIFs and Sema3G protein levels, related to Figure 7**C** (n = 3 independent experiments). (**D-G**) Immunoblot analysis of Sema3G and HIFs expression in bEnd.3 cells, which were transfected with siHIF-1α (**D** and **E**), siHIF-2α (**F** and **G**), or siControl for 48 h and then exposed to hypoxia (1% O_2) for an additional 12 h (n = 3 independent experiments). Error bars represent mean ± SEM. *P<0.05; **P<0.01; ***P<0.001; 2-tailed Student's t tests.

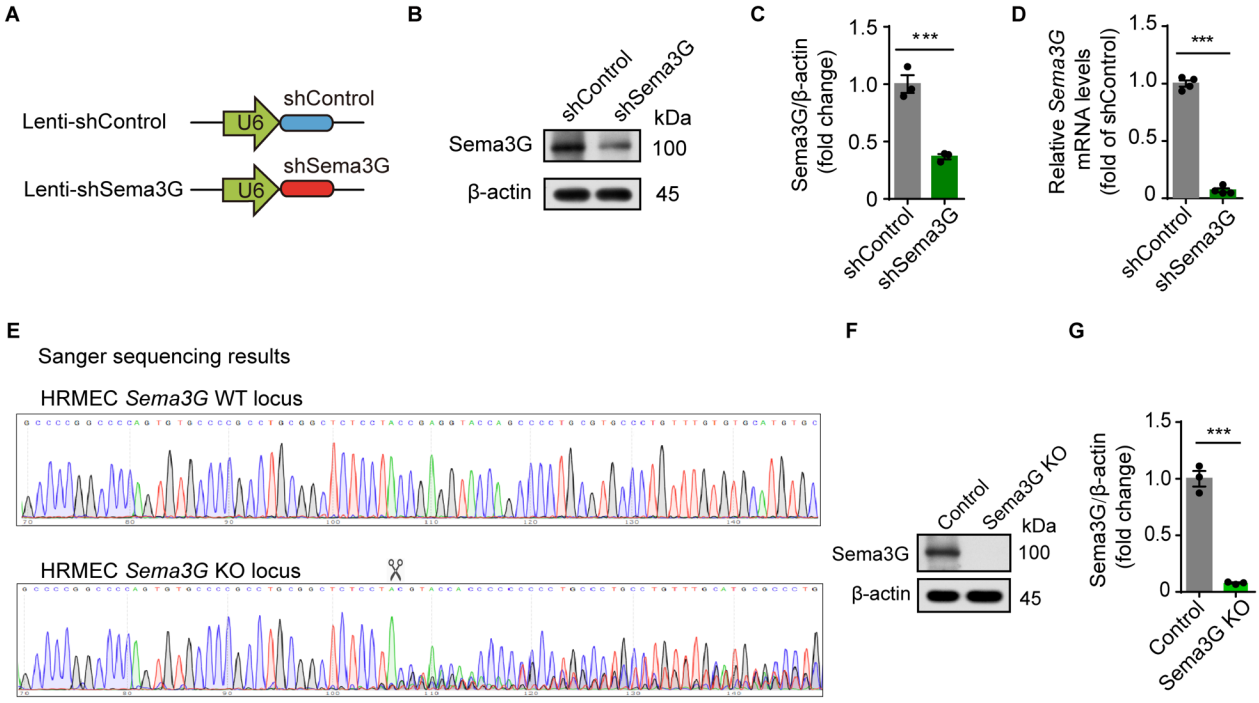

Supplemental Figure 9. RNA interference-mediated Sema3G knockdown and CRISPR/Cas9-mediated Sema3G deletion in HRMECs. (**A**) Diagram of shControl and shSema3G lentivirus. (**B** and **C**) Immunoblot analysis and quantification of Sema3G protein levels in HRMECs transfected with shControl and shSema3G lentivirus (n = 3 independent experiments). (**D**) Analysis of *Sema3G* mRNA levels by RT-qPCR in shControl and shSema3G HRMECs (n = 4 independent experiments). (**E**) DNA sequencing of PCR products amplified from the genome of control or Sema3G-KO HRMECs was aligned to the *Sema3G* reference sequence. Many overlapping peaks were present at CRISPR/Cas9 targeting site in the sequencing results, indicating effective gene editing for Sema3G. (**F** and **G**) Immunoblot analysis and quantification of Sema3G protein levels in control and Sema3G-KO HRMECs to confirm depletion of Sema3G (n = 3 independent experiments). Error bars represent mean ± SEM. ***P < 0.001; 2-tailed Student's t tests.

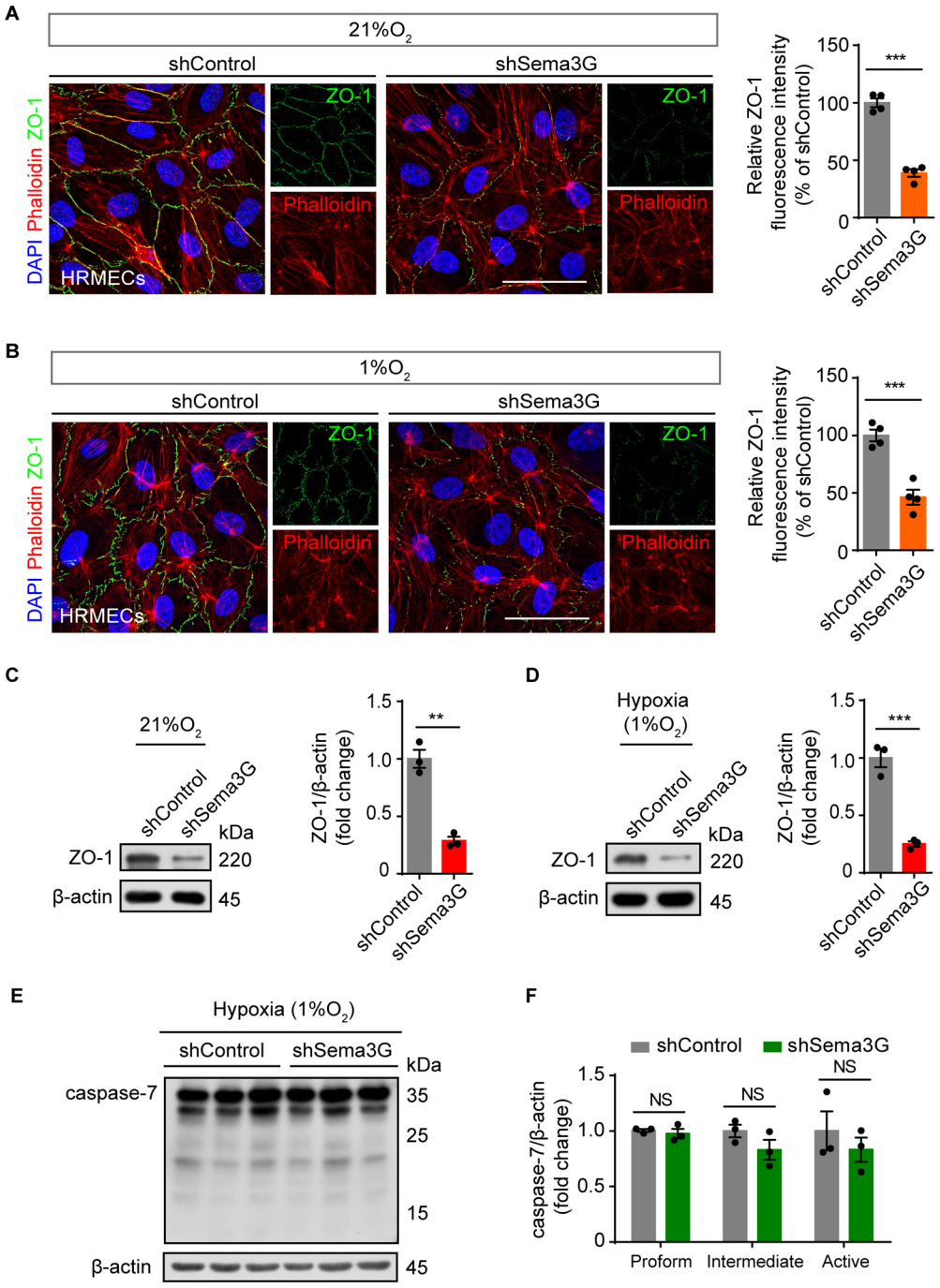

Supplemental Figure 10. Loss of Sema3G impairs tight junction distribution in ECs. (**A** and **B**) Confocal images of shControl or shSema3G-treated HRMECs exposed to normoxia (**A**, 21% O_2) or hypoxia (**B**, 1% O_2) stained with ZO-1 (green) and phalloidin (red). Fluorescence signal intensities of ZO-1 staining quantified from **A** and **B** (right panel, n = 4 independent experiments for each group). (**C** and **D**) Immunoblot analysis and quantification of ZO-1 protein levels in HRMECs transfected with shControl or shSema3G lentivirus and exposed to normoxia (**C**, 21% O_2) or hypoxia (**D**, 1% O_2) (n = 3 independent experiments for each group). (**E** and **F**) Sema3G knockdown did not induce cell death or apoptosis, as determined by assessment of caspase-7 activation (n = 3 independent experiments for each group). Error bars represent mean ± SEM. **P<0.01, ***P<0.001; 2-tailed Student's t tests. Scale bars: 50 μm (**A** and **B**).

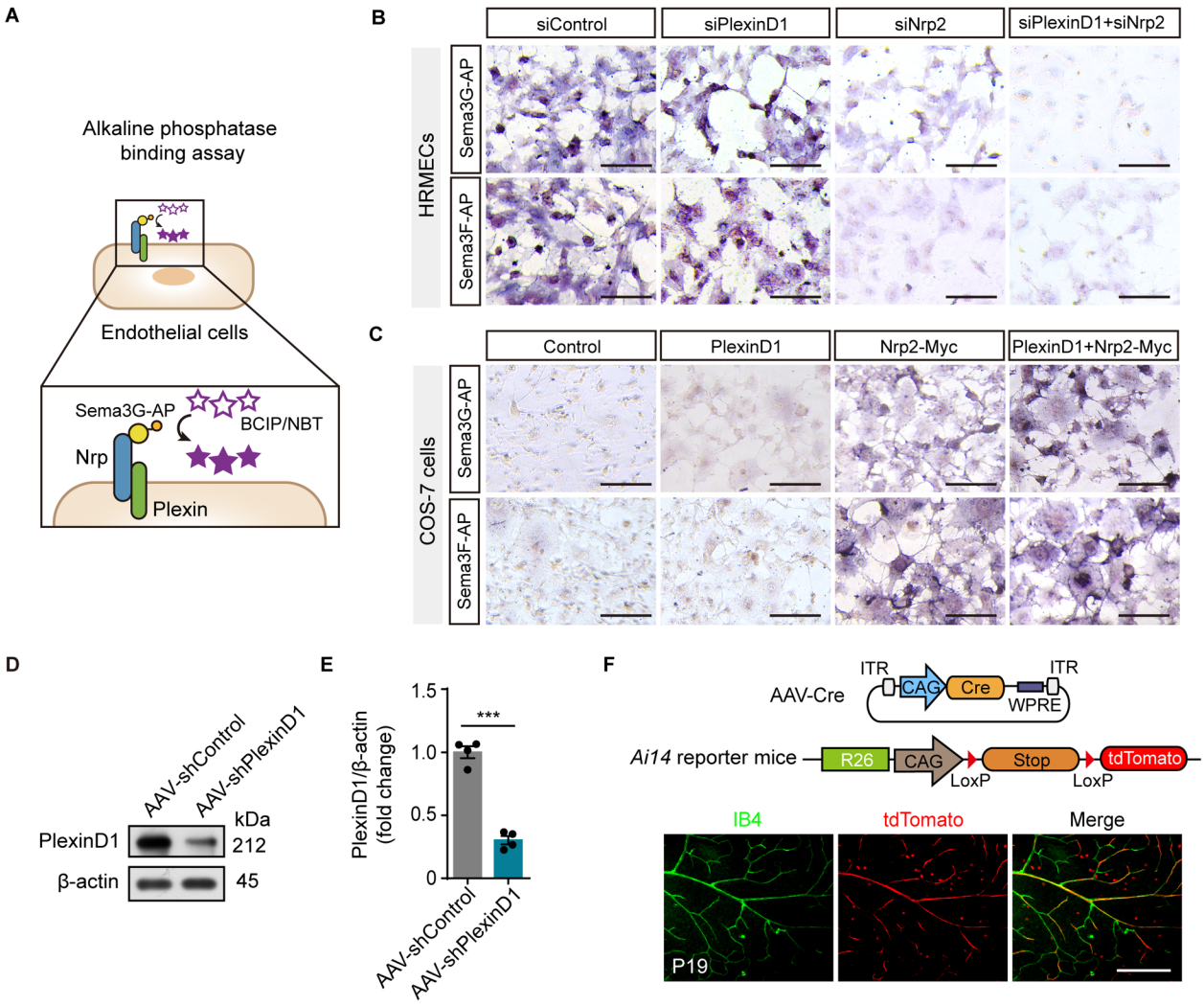

Supplemental Figure 11. Sema3G binds to the Nrp2/PlexinD1 complex in vitro. (**A**) Schematic illustration of the alkaline phosphatase (AP)-tagged ligand binding experiment. The cells were incubated with AP-tagged ligands, rinsed, and then processed for the detection of AP binding using 5-bromo-4-chloro-3-indolyl-phosphate (BCIP)/nitroblue tetrazolium (NBT) substrate solution. (**B**) AP-Sema3G or AP-Sema3F binding on the surface of HRMECs, which were transfected with siControl, siPlexinD1 alone, siNrp2 alone, or siPlexinD1 with siNrp2, was colorimetrically measured by BCIP/NBT. (**C**) AP-Sema3G or AP-Sema3F binding on the surface of COS-7 cells, which were transfected with control, PlexinD1 alone, Nrp2 alone, or PlexinD1 with Nrp2 overexpression vectors, was colorimetrically measured by BCIP/NBT. (**D** and **E**) Immunoblot analysis and quantification of PlexinD1 protein in retinas of OIR mice transfected with AAV-shControl or AAV-shPlexinD1 (n = 4 independent experiments). (**F**) Verification of AAV transduction efficiency in Cre-dependent *Ai14* reporter mice. Neonatal *Ai14* mice were injected through the retro-orbital sinus and infected with AAV carrying Cre recombinase at P7 and P12. The retinas were analyzed at P19. tdTomato was robustly expressed in retinal ECs of *Ai14* mice following Cre-mediated recombination. Error bars represent mean ± SEM. ***P<0.001; 2-tailed Student's t tests. Scale bars: 100 μm (**B** and **C**) and 200 μm (**F**).

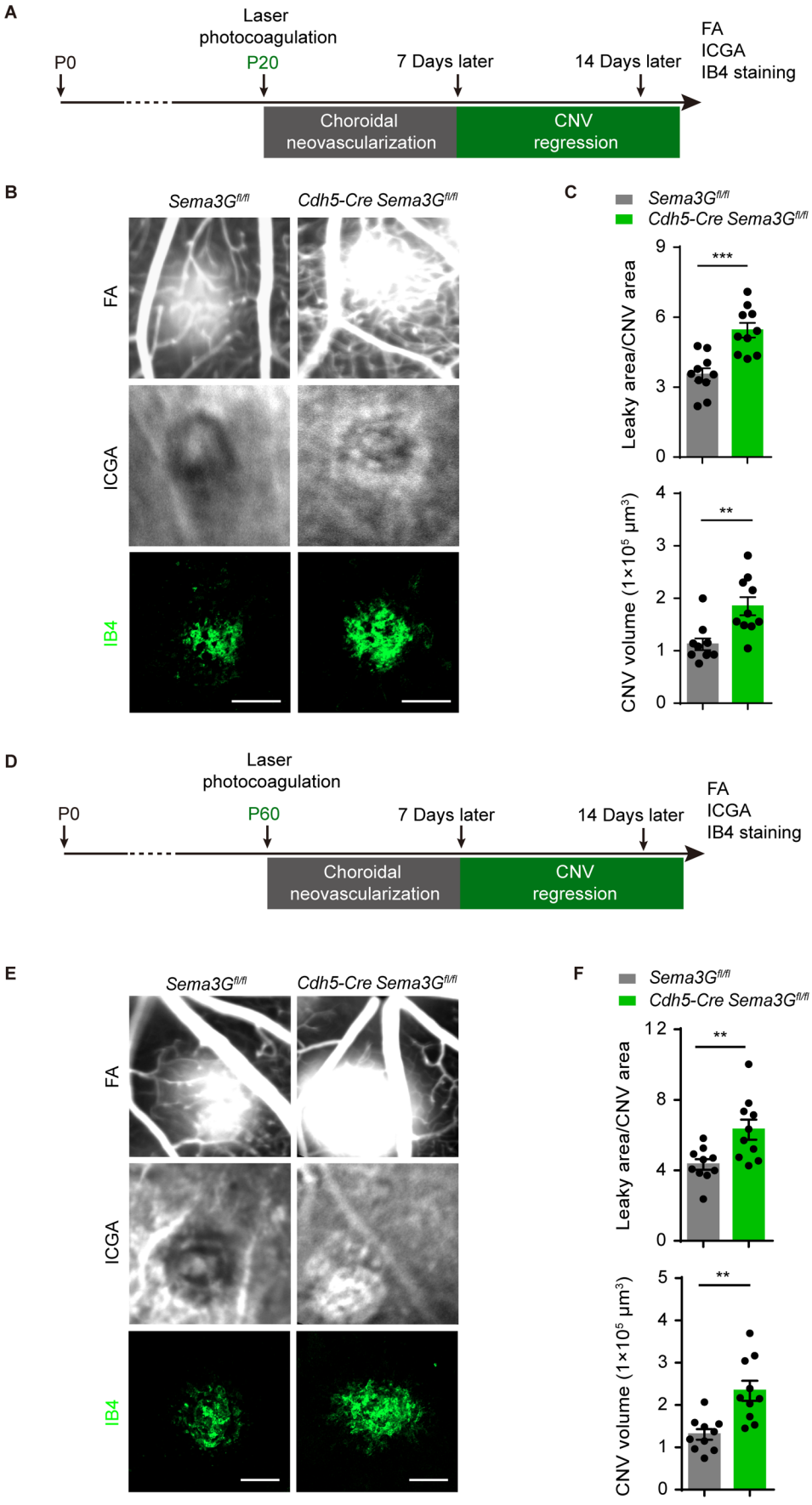
A
Laser photocoagulation
P0
P20
7 Days later
14 Days later
FA
ICGA
IB4 staining
Choroidal neovascularization
CNV regression
B
Sema3G fl/fl
Cdh5-Cre Sema3G fl/fl
FA
ICGA
IB4
C
Sema3G fl/fl
Cdh5-Cre Sema3G fl/fl
Leaky area/CNV area
***
CNV volume (1×10⁵ μm³)
**
D
Laser photocoagulation
P0
P60
7 Days later
14 Days later
FA
ICGA
IB4 staining
Choroidal neovascularization
CNV regression
E
Sema3G fl/fl
Cdh5-Cre Sema3G fl/fl
FA
ICGA
IB4
F
Sema3G fl/fl
Cdh5-Cre Sema3G fl/fl
Leaky area/CNV area
**
CNV volume (1×10⁵ μm³)
**

Supplemental Figure 12. Endothelial Sema3G is required for pathological vessel regression in CNV models. (**A** and **D**) *Sema3G*$^{fl/fl}$ and *Cdh5-Cre Sema3G*$^{fl/fl}$ mice were treated with laser photocoagulation at P20 (**A**) or P60 (**D**). The degree of CNV was evaluated with fluorescein angiography (FA), indocyanine green angiography (ICGA) and IB4 staining at 2 weeks after photocoagulation treatment. (**B** and **E**) Vascular leakage was assessed by FA, and the extent of CNV was assessed by ICGA followed by labeling of flat-mounted choroids with IB4 in *Sema3G*$^{fl/fl}$ and *Cdh5-Cre Sema3G*$^{fl/fl}$ CNV mice. (**C** and **F**) Leaky areas from CNV was calculated as hyperfluorescent areas in FA images divided by CNV areas in ICGA images, and CNV volumes were measured by IB4-positive neovascular volume in *Sema3G*$^{fl/fl}$ and *Cdh5-Cre Sema3G*$^{fl/fl}$ mice (**C**, P20, n = 10 mice for each group; **F**, P60, n = 10 mice for each group). Error bars represent mean ± SEM. **P<0.01; ***P<0.001; 2-tailed Student's t tests. Scale bars: 100 μm (**B** and **E**).

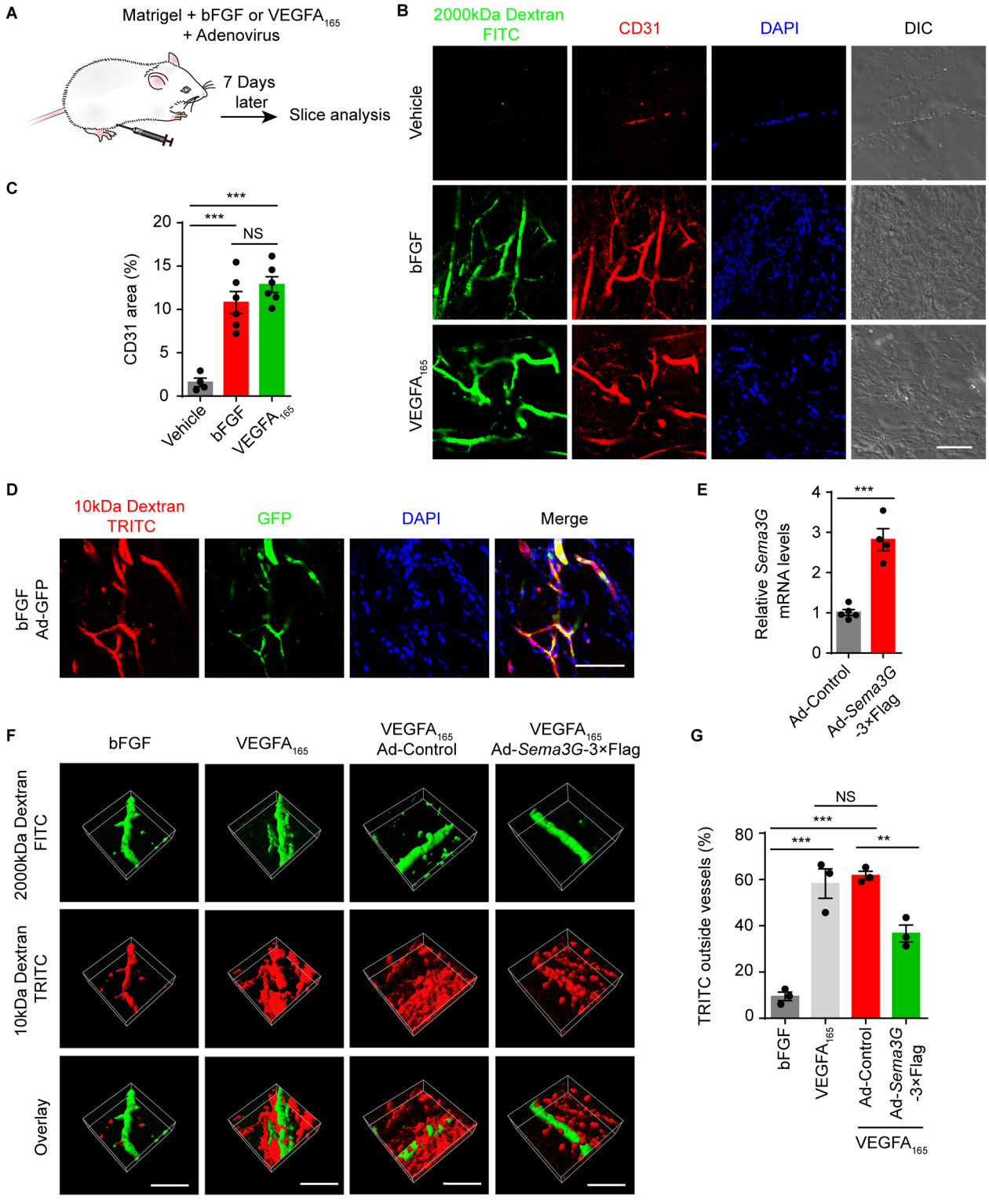
A
Matrigel + bFGF or VEGFA165
+ Adenovirus
7 Days
later
Slice analysis
B
2000kDa Dextran
FITC
CD31
DAPI
DIC
Vehicle
bFGF
VEGFA165
C
CD31 area (%)
***
***
NS
Vehicle
bFGF
VEGFA165
D
10kDa Dextran
TRITC
GFP
DAPI
Merge
bFGF
Ad-GFP
E
Relative Sema3G
mRNA levels
***
Ad-Control
Ad-Sema3G
-3×Flag
F
bFGF
VEGFA165
VEGFA165
Ad-Control
VEGFA165
Ad-Sema3G-3×Flag
2000kDa Dextran
FITC
10kDa Dextran
TRITC
Overlay
G
TRITC outside vessels (%)
NS
***
***
**
bFGF
VEGFA165
Ad-Control
Ad-Sema3G
-3×Flag
VEGFA165

Supplemental Figure 13. Sema3G overexpression prevents VEGFA-induced vascular leakage in vivo. (**A**) Schematic illustration of the in vivo Matrigel angiogenesis assay. Mice received a subcutaneous injection of Matrigel supplemented with bFGF alone, $VEGFA_{165}$ alone or $VEGFA_{165}$ with adenovirus (Ad-Control or Ad-Sema3G-3 × Flag). (**B** and **C**) Perfused vessels were quantified by measuring the area of dextran-FITC and CD31 staining within the Matrigel plug on day 7 after injection (n = 4, 6, 6 mice). (**D**) Representative images of 10 kDa dextran-TRITC-perfused vessels (red) infected by the adenovirus expressing GFP (green) in Matrigel sections. (**E**) *Sema3G* mRNA levels were analyzed by RT-qPCR in the Matrigel plugs harvested from the Ad-Control groups and the Ad-Sema3G-3 × Flag groups on day 7 after injection (Ad-Control, n = 5 mice; Ad-Sema3G-3 × Flag, n = 4 mice). (**F**) 3D rendering of confocal microscopy images of perfused vessels with dextran tracers in Matrigel plugs sections. (**G**) Vessel permeability was quantified by measuring the area of 10 kDa dextran-TRITC present outside of the 2000 kDa dextran-FITC positive vessels (n = 3 mice for each group). Error bars represent mean ± SEM. **P<0.01; ***P<0.001; 2-tailed Student's t tests (**E**) and 1-way ANOVA with Tukey's multiple comparisons test (**C** and **G**). Scale bars: 100 μm (**B** and **D**) and 50 μm (**F**).

Supplemental Table 1. Clinical characteristics of patients having undergone vitreous biopsy (related to Figure 2, B-D).

Sample	Sex	Age (Years)	Patient conditions	Analysis
C1	Male	72	ERM	ELISA/WB
C2	Male	65	ERM	ELISA/WB
C3	Female	72	MH	ELISA/WB
C4	Female	70	ERM	ELISA
C5	Female	72	MH	ELISA
C6	Female	67	ERM	ELISA
C7	Female	69	MH	ELISA
C8	Female	72	MH	ELISA
C9	Female	68	MH	ELISA
C10	Female	56	MH	ELISA
D1	Female	68	PDR	ELISA/WB
D2	Female	44	PDR	ELISA/WB
D3	Male	56	PDR	ELISA/WB
D4	Male	69	PDR	ELISA
D5	Female	60	PDR	ELISA
D6	Female	51	PDR	ELISA
D7	Female	47	PDR	ELISA
D8	Male	35	PDR	ELISA
D9	Male	66	PDR	ELISA
D10	Male	71	PDR	ELISA

C indicates control (nonvascular pathology); D, diabetes; PDR, proliferative diabetic retinopathy; ERM, idiopathic epiretinal membrane; MH, idiopathic macular hole; WB, western blot; and ELISA, enzyme-linked immunosorbent assay.

Supplemental Table 2. Clinical characteristics of patients having undergone intravitreal anti-VEGF drug injection or cataract surgery (related to Figure 2, E and F).

Sample	Sex	Age (Years)	Patient conditions	Analysis
Control 1	Female	68	cataract surgery	WB
Control 2	Male	57	cataract surgery	WB
Control 3	Male	64	cataract surgery	WB
PDR without DME 1	Female	67	PDR (no DME)	WB
PDR without DME 2	Female	39	PDR (no DME)	WB
PDR without DME 3	Female	54	PDR (no DME)	WB
PDR with DME 1	Male	49	PDR (DME)	WB
PDR with DME 2	Female	55	PDR (DME)	WB
PDR with DME 3	Male	70	PDR (DME)	WB
DME only 1	Male	62	DME	WB
DME only 2	Male	48	DME	WB
DME only 3	Male	60	DME	WB

Control indicates nondiabetic patients who had undergone cataract surgery; PDR, proliferative diabetic retinopathy; DME, diabetic macular edema; and WB, western blot.

Supplemental Table 3. Body weights (g) of mice.

Developmental stage

	P5	n	P6	n	P10	n
Sema3G$^{fl/fl}$	3.1±0.18	11	3.5±0.09	28	5.1±0.15	12
Cdh5-Cre Sema3G$^{fl/fl}$	3.0±0.10	11	3.3±0.08	27	5.2±0.14	12
	P14	n	P20	n	P60	n
Sema3G$^{fl/fl}$	6.9±0.12	5	10.4±0.11	27	22.9±0.53	16
Cdh5-Cre Sema3G$^{fl/fl}$	6.9±0.11	5	10.4±0.08	27	22.7±0.52	16

OIR (related to Figure 6, A-J, and Figure 9, A-B)

	P13	n	P15	n	P17	n	P19	n
Sema3G$^{fl/fl}$	5.4±0.09	10	5.9±0.11	8	6.5±0.10	8	7.3±0.08	25
Cdh5-Cre Sema3G$^{fl/fl}$	5.2±0.09	10	5.9±0.07	8	6.6±0.14	8	7.3±0.09	25

OIR (related to Figure 10, C-F)

	P19	n
Sema3G$^{fl/fl}$ + NaCl	7.4±0.11	11
Cdh5-Cre Sema3G$^{fl/fl}$ + NaCl	7.2±0.12	11
Sema3G$^{fl/fl}$ + LiCl	7.2±0.09	11
Cdh5-Cre Sema3G$^{fl/fl}$ + LiCl	7.3±0.15	11

OIR (related to Figure 12, E-G)

	P19	n
Cdh5-Cre Sema3G$^{fl/fl}$ + AAV-shControl + lgG	7.2±0.07	9
Cdh5-Cre Sema3G$^{fl/fl}$ + AAV-shControl + Sema3G	7.3±0.15	10
*Cdh5-Cre Sema3G$^{fl/fl}$ +AAV-sh*PlexinD1 + *lgG*	7.4±0.15	8
*Cdh5-Cre Sema3G$^{fl/fl}$ +AAV-sh*PlexinD1 + *Sema3G*	7.3±0.13	10

OIR (related to Figure 13, E-G)

	P19	n
Sema3G$^{fl/fl}$ + AAV-Control	7.2±0.08	8
Sema3G$^{fl/fl}$ + AAV-Sema3G	7.3±0.11	10
Cdh5-Cre Sema3G$^{fl/fl}$ + AAV-Control	7.1±0.12	9
Cdh5-Cre Sema3G$^{fl/fl}$ + AAV-Sema3G	7.3±0.08	9

OIR (related to Figure 13, K-M)

	P17	n
Sema3G$^{fl/fl}$ + lgG	6.3±0.08	10
Sema3G$^{fl/fl}$ + Sema3G	6.4±0.08	10
Cdh5-Cre Sema3G$^{fl/fl}$ + lgG	6.5±0.09	10
Cdh5-Cre Sema3G$^{fl/fl}$ + Sema3G	6.4±0.07	10

P, postnatal day. *n*, number of mice. No significant differences in body weight were observed between *Sema3G$^{fl/fl}$* and *Cdh5-Cre Sema3G$^{fl/fl}$* mice. In addition, the treatments in each groups had no effects on body weight of mice with OIR. Values are mean ± SEM.

Supplemental Table 4. Primer sets used for RT-qPCR.

Gene	Species	Forward (5'-3')	Reverse (5'-3')
Sema3A	Mus	CACTGGGATTGCCTGTCTT	GGCCAAGCCATTAAAAGTGA
Sema3B	Mus	CTTCGGCTCTCCTTTCAAGA	CAAGGCTTCATAACAGCAGGT
Sema3C	Mus	ATCTGGCAAAGGACGATGCTCTTT	GTGCGTCCACAAACATGGGTTCAC
Sema3D	Mus	ACCATCGCTGGGTGCAATAT	GGGTGCCGCCTTATGAAAC
Sema3E	Mus	TCAGTGACGGCTACAGAGAGA	CACACTCATTTGCGTCTTTTCC
Sema3F	Mus	TCGCGCACAGGATTACATCTT	ACCGGGAGTTGTACTGATCTG
Sema3G	Mus	GCCAGAGCCAAAACAAAGCAG	AGTGTAGTTTCCTGCGTCATGG
VEGFA	Mus	TTCATGGATGTCTACCAGCGAAGCTACT	TCTGCTGTGCTGTAGGAAGCTCATCTC
GAPDH	Mus	CGTCCCGTAGACAAAATGGT	TTGATGGCAACAATCTCCAC
Sema3G	Homo	CTCAAAGTCATCGCTCTCCAGGC	AGTGCCGTAAGTCTCACATTGG
GAPDH	Homo	TTTGGTCGTATTGGGCGCCTGG	CTCAGCCTTGACGGTGCCATGG

Supplemental Table 5. Primer sets used for ChIP-qPCR.

Gene	Species	sites	Forward (5'-3')	Reverse (5'-3')
Sema3G	Mus	ChIP-1	TGGGTGTTCAGCTCAATCTC	CATTCTGCATCTACCTCCCTG
Sema3G	Mus	ChIP-2	AGCAGAGCAAACTACATCCAG	ACATGGAACAGAAGGCTCC

Supplemental Table 6. Targeting sequences for RNA interference.

Gene	Species	Targeting sequences (5'-3')
Sema3G	Homo	GCGGGUGCUGGUGAACAAA
Nrp2	Homo	AGAUUGUCCUCAACUUCAA
PlexinD1	Homo	GCACUUCCUCAUCGUCUUU
PlexinD1	Mus	GCAAGAAAGUAUUGCCAGA
HIF1a	Mus	CUCCAAGUAUGAGCACAGU
HIF2a	Mus	CAGUGACGAUGUGGCUGUAACUGAG
Negative control	/	UUCUCCGAACGUGUCACGU

Supplemental Table 7. sgRNA guide sequences to target human Sema3G.

Gene	**Species**	**Targeted genomic locus (5'-3')**	**sgRNA sequence (5'-3')**
Sema3G	Homo	CGCCTGCGGCTCTCCTACCG**AGG**	CGCCUGCGGCUCUCCUACCG
Negative control	/	TTCTCCGAACGTGTCACGT**CGG**	UUCUCCGAACGUGUCACGU

Supplemental Table 8. Primer sets used for sequencing analysis of genome modification.

Gene	Species	Forward (5'-3')	Reverse (5'-3')
Sema3G	Homo	CGGGACCAGAGGGCGGCTCTG	GCCTCCCACCGCCACCCTGGTC